Journal of Materials and Environmental Sciences
ISSN : 2028-2508
CODEN : JMESCN

J. Mater. Environ. Sci., 2019, Volume 10, Issue 1, Page 15-21

http://www.jmaterenvironsci.com

Box-Behnken-optimized Cu(I) photo-Fenton-like degradation of Basic Violet 3

A. Abubakar, U.I. Gaya*

Department of Pure and Industrial Chemistry, Bayero University, Kano.

Received 25 Feb 2019,
Revised 11 April 2019,
Accepted 13 April 2019

Keywords
- ✓ Photo-Fenton-like,
- ✓ Box-Behnken,
- ✓ Degradation,
- ✓ Cu(I),
- ✓ Basic Violet 3.

uigaya.chm@buk.edu.ng;
Phone: +2348039169418;
Fax: +23464665904

Abstract

The homogeneous oxidative photodegradation of Basic Violet 3 in presence of Cu^{+}/H_2O_2 is reported. The effects of operating variables such as pH, $[H_2O_2]$, $[Cu^{+}]$ and [Dye] were maximized with the aid of Box-Behnken design. The dye removal was monitored by using UV-visible spectrophotometer, Fourier transform infra-red spectroscopy (FTIR) and total carbon analyzer. The degradation efficiency for Basic Violet (BV3) reached 99% and appreciable mineralization (70 %) was achieved. Kinetic profiles show consistency with pseudo-first-order rate scheme. Evidence for phenyl ring opening was corroborated by FTIR spectroscopy. The Cu(I) photo-Fenton-like degradation is favored by increasing pH.

1. Introduction

Dyes are constantly in the forefront as major, widespread and toxic aqueous environmental pollutants. A significant proportion of the textile dyes remain unfixed to the fabrics, thus leading to large amounts being released into the industrial effluents [1,2]. Among all synthetic dyes, basic dyes are the most brilliant but they lack light and wash fastness. Nonetheless, these dyes have widespread application in antiseptic, cosmetic, food, paper coloring, and textile industries. The polyaromatic frame of basic dye structure is perhaps a culprit for their toxic and non-biodegradable nature [3]. Basic Violet 3 (BV3) is non-biodegradable dyestuff, mutagen, mitotic poison and potent carcinogen, toxic to mammalian cells and persistent in many environments [4,5]. Advanced oxidation processes are efficient pollutant removal methods that yield environmentally-friendly products. Photo-Fenton is a member of the advanced oxidation process, which rely on powerful in situ-generated hydroxyl radicals to degrade organic pollutants [6]. The Fenton reagent is a chemical system consisting usually of iron (II) salts or oxide, and hydrogen peroxide. Various Fenton or Fenton-like systems have been utilized for the removal of basic dyes. Basic Violet 10 has been decontaminated by coupling Fenton with sonication [7] or electric bias [8].

The degradation of BV3 by the photo-Fenton process has recently been described [5]. One of the disadvantages of Fenton and photo-Fenton processes is the need for iron salts [9]. Consequently, there is intensive interest in Fenton-like systems. Recently, attention has been geared towards the utilization of Cu(II)/Cu(I) Fenton-like systems for their impeccable efficiency [10]. Similarly, Basic Violet has been removed by a photo-Fenton-like reactivity system based on Fe(III) and H_2O_2 [11]. Herein, the degradation of Basic Violet in an irradiated Fenton-like system of Cu(I) + H_2O_2 is for the first time investigated.

2. Material and Methods

2.1. Chemicals

The chemicals used in this study include Basic Violet 3 (99 %; CAS 548-62-9), copper (I) nitrate (99 %), H_2SO_4 (98 %) and H_2O_2 (30 % w/v) from Sigma-Aldrich. Sodium hydroxide (99 %) was obtained from BDH. The structure of Basic Violet 3 is shown in Figure 1. Solutions of these chemicals were prepared using deionized water without further purification.

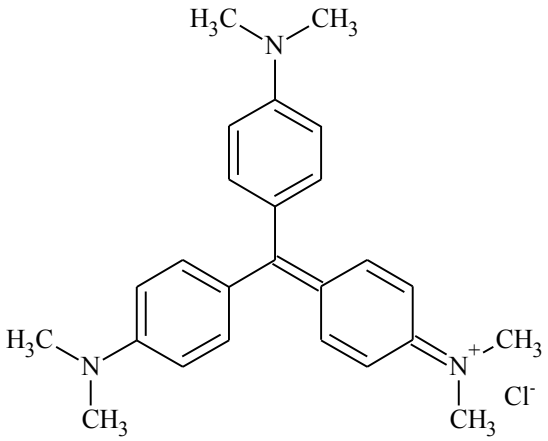

Figure 1 : Structure of Basic Violet 3.

2.1. Photo-Fenton-like experiments

In order to maximize the removal of BV3 the photo-Fenton-like process, twenty nine experiments were performed based on Box-Behnken design, using Design Expert v6. This design method consists of a rotatable, quadratic frame having no embedded factorial or fractional factorial points where the factor combinations are at the midpoints of the edges of the factor space and at the center. In this study, experiments were based on four independent variables (pH, Cu^{+} dosage, H_2O_2 and initial BV3 concentration) combined at three levels. The input levels of these variables with their codes are shown in Table 1.

Table1: Input levels and codes of variables.

Variables	Levels (and Codes)		
A-pH	1 (-1)	5.5(0)	11(+1)
B-H_2O_2 (mg/L)	20(-1)	60(0)	120(+1)
C-Cu^{+} (mg/L)	5(-1)	15(0)	30(+1)
D-Dye (mg/L)	10(-1)	30(0)	60(+1)

Photo-Fenton-like experiments were performed in a 500 ml borosilicate batch reactor installed with 2000 Wm^{-2} halogen lamp. Aliquots of the stock of dye solution, $CuNO_3$ and H_2O_2 were taken (in accordance with the input levels in Table 1) and added into the reactor. The volume was made up to 500 ml and irradiation was performed. Samples were taken at the intervals of 0, 20, 50, 80, 120, 140, 160, 180, 200 and 220 min. The progress of the degradation process was monitored by performing UV-Visible spectrometry at 580 nm using a Perkin Elmer Lambda 25 UV-visible spectrophotometer. The percent degradation ($\% D_{exp}$) of the dyes was calculated using equation (1).

$$\% D_{\exp} = 1 - \left(\frac{C_t}{C_0}\right) \text{ x } 100 \qquad (1)$$

Where C_o is the initial concentration of the dye, C_t is the concentration of BV3 at a given time t. The progress of the mineralization process was monitored by the measurements of total organic carbon (TOC) by the used of Shimadzu 00077 TOC analyzer before and after the mineralization process at regular intervals. The extent of mineralization of each dye was calculated using equation (2).

$$\% \text{ Mineralization} = 1 - \frac{TOC_t}{TOCo} \text{ x } 100 \qquad (2)$$

Where TOC_0 is the total organic carbon before mineralization and TOC_t is the total organic carbon at a given time t. The changes in the BV3 functional groups were observed using Fourier transform infrared spectroscopy. The analysis was carried out on the dye samples before and after degradation using Thermo-Scientific Nicolet iS10 FT-IR spectrometer operated in the range of 4000 to 650 cm^{-1}. At the other end, the kinetic scheme for copper (I) homogeneous photo-Fenton degradation of BV3 was evaluated after the first 20 min of reaction using optimized values and data were fitted into kinetic models.

The effect of operating parameters (initial BV3 concentration, H_2O_2, Cu^+ or solution pH) was studied with the aid of response surfaces obtained from Box-Behnken experiments. In addition, the effect of the presence of oxidizing agents such as $KClO_3$ and $KBrO_3$ was studied in concentrations of 0, 50, 150, 200, 250 mg/L.

3. Results and discussion

The values of BV3 degradation efficiency obtained from photo-Fenton-like experiment (% D) were processed using Box-Behnken design to obtain statistically valid predicted values (% D_{pred}). These values are listed in Table 2. This experimental design method requires fewer runs than the majority of others [12].

Table 2: Actual values of BV3 degradation efficiencies along with the predicted values.

Run	A:pH	B:H_2O_2	C:Cu(I)	D: BV3	% D_{exp}	% D_{pred}
1	1.00	0.00	-1.00	0.00	80	78.74
2	1.00	0.00	0.00	-1.00	85	96.56
3	0.00	0.00	0.00	0.00	68	71.68
4	0.00	0.00	0.00	0.00	80	71.68
5	-1.00	0.00	-1.00	0.00	32	41.44
6	0.00	1.00	-1.00	0.00	45	38.91
7	0.00	0.00	0.00	0.00	80	71.68
8	0.00	1.00	0.00	-1.00	50	56.73
9	-1.00	0.00	0.00	-1.00	50	59.23
10	1.00	-1.00	0.00	0.00	95	90.95
11	0.00	0.00	1.00	1.00	60	63.69
12	0.00	-1.00	0.00	-1.00	70	66.06
13	1.00	0.00	0.00	1.00	99	96.56
14	0.00	-1.00	-1.00	0.00	48	48.24
15	0.00	1.00	0.00	1.00	50	56.73
16	0.00	0.00	1.00	-1.00	55	63.69
17	0.00	0.00	0.00	0.00	82	71.68
18	0.00	0.00	-1.00	1.00	60	53.85
19	0.00	1.00	1.00	0.00	50	48.74
20	0.00	0.00	-1.00	-1.00	50	53.85
21	0.00	-1.00	1.00	0.00	55	58.07
22	-1.00	1.00	0.00	0.00	52	56.73
23	0.00	0.00	0.00	0.00	65	71.68
24	1.00	0.00	1.00	0.00	94	88.57
25	1.00	1.00	0.00	0.00	80	81.61
26	-1.00	-1.00	0.00	0.00	50	53.61
27	0.00	-1.00	0.00	1.00	65	66.06
28	-1.00	0.00	0.00	1.00	65	59.23
29	-1.00	0.00	1.00	0.00	60	51.24

Both the experimental and predicted efficiencies show a good correlation as corroborated by the outstanding linear correlation of normal probabilities with studentized residuals. However, because the BV3 concentration term D, the cross terms AB, AC, *AD*, *BC*, *BD*, *CD* and the square term D^2 do not support the model hierarchy, the degradation model is a reduced quadratic type shown in equation (3). Consequently, the operating variables can be said to influence the efficiency of the Fenton-like photodegradation process within the ranges of this study except for the initial BV3 concentration.

$$\%\ D_{pred} = 71.68 + 18.67A - 4.67B + 4.92C + 6.22A^2 - 10.28B^2 - 12.91C^2 \quad (3)$$

From the table, the optimum photo-Fenton-like degradation efficiency (99 %) corresponds to pH 11, 60 mg/L H_2O_2, 15 mg/l Cu(I). This is a bit higher than the efficiency (97.5 %) reported for a Box-Behnken designed

photo-Fenton removal of Direct Red 28 [13]. Of special note is that unlike in the case of photo-Fenton where the pH must be acidic to avoid precipitation of iron(III) hydroxide [14], the photo-Fenton-like process in this study performed best at pH 11.

The analysis of variance of the reduced quadratic model applicable to this study is displayed in Table 3. From the Table, the F-values of the model and model terms A, B, C, A^2, B^2 and C^2 are > 4 which indicates low chances of noise and confirms the significance of the quadratic model. This is further corroborated by the values of Prob > F which are all < 0.05 less. The lack of fit of 0.6715 is not significant relative to the pure error which promises good model fit

Table 3: Analysis of variance for of the response surface quadratic model.

Source	Sum of squares	DF	Mean square	F-value	Prob > F	Remark
Model	6942.18	6	1157.03	22.20	< 0.0001	Significant
A	*4181.33*	*1*	*4181.33*	*80.24*	*< 0.0001*	
B	*261.33*	*1*	*261.33*	*5.02*	*0.0356*	
C	*290.08*	*1*	*290.08*	*5.57*	*0.0276*	
A^2	*260.23*	*1*	*260.23*	*4.99*	*0.0359*	
B^2	*710.98*	*1*	*710.98*	*13.64*	*0.0013*	
C^2	*1120.42*	*1*	*1120.42*	*21.50*	*0.0001*	
Residual	1146.37	22	52.11	*0.80*	*0.6715*	
Lack of Fit	*898.37*	*18*	*49.91*			Not significant
Pure Error	*248.00*	*4*	*62.00*			
Cor Total	8088.55	28				

Table 4 shows some statistics of dispersion associated with the BV3 degradation model. From the Table, the PRESS value of the model of 1938.88 indicates a high signal-to-noise ratio. Another measure of the signal-to-noise ratio is adequate precision. The minimum adequate precision desirable in any experiment is a value > 4. In this study, the adequate precision is 16.257 and that describes good model discrimination. The value of adjusted R-squared (0.8196) is in good agreement with that of the predicted R-squared (0.7603).

Table 3: Summary of analysis of variance (ANOVA) statistics for BV3 Box-Behnken photo-Fenton-like experimental design

Statistical parameter	Value
Std.dev	7.14
Mean	64.66
C.V%	11.16
PRESS	1938.88
R-squared	0.8583
Adj.R-squared	0.8196
Pred.R-squared	0.7603
Adequate precision	16.257

The response surface plots showing the effect of operating parameters are displayed in Figure 2. Figure 2a shows the effect of H_2O_2 addition vis-à-vis pH. From the figure, the photo-Fenton-like degradation increases with either of pH or H_2O_2. However, even with little hydrogen peroxide, pH can bring significant photo-Fenton-like degradation up to 94 %. The response surface (Figure 2b) shows that only a moderate combination of H_2O_2 concentration and Cu(I) is required to provide the best synergism. At the other end, the response surface showing the interplay between BV3 and H_2O_2 concentration (Figure 3c) shows no influence of the dye on the photo-Fenton-like efficiency.

Certain anions such as phosphate were found to dramatically inhibit the Fenton-mediated decoloration of the BV3 [15]. In this study, the effect of the presence of oxidizing agents such as ClO_3 and BrO_3 was studied in concentrations of 0, 50, 150, 200, 250 mg/L. The results depicted in Figure 3 shows that the addition of electron recipient species has no influence on the photo-Fenton performance of the Cu(I) process.

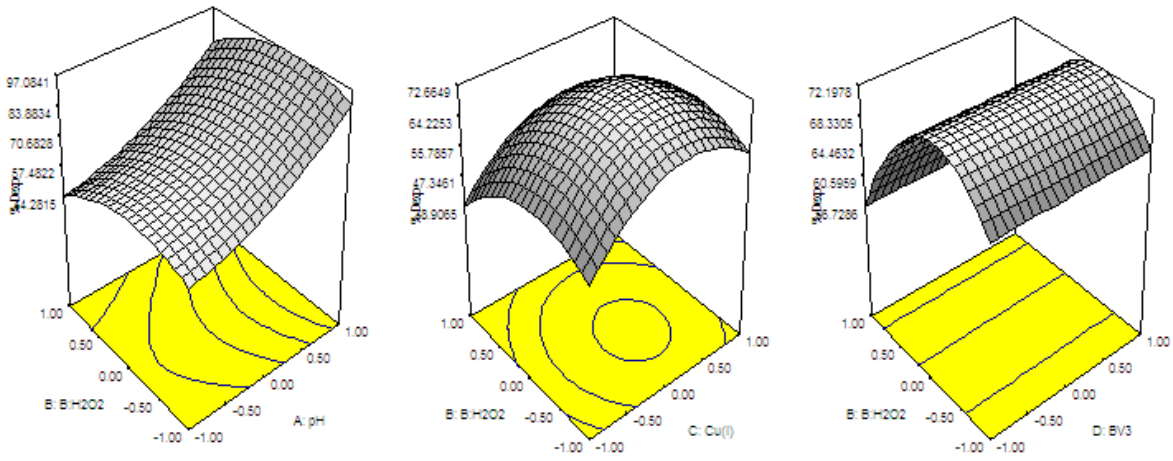

Figure 2: Response surface plots showing the interaction of H_2O_2 with (a) pH (b) Cu(I) doses (c) BV3 initial concentration.

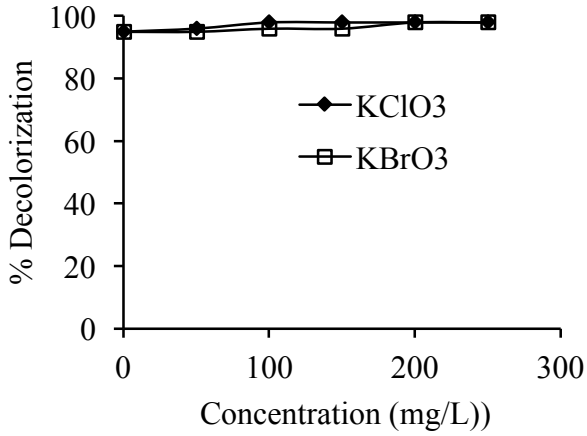

Figure 3: A graph showing the effect of electron recipients on the degradation of BV3 at the optimum pH, H_2O_2, Cu^+ and BV3 concentrations.

Even though 99% of BV3 has been degraded, mineralization, which is the most desirable, may not be as effective. In this study, mineralization has was monitored based on TOC measurement and the results of this study are shown in Figure 4. As seen from the figure, the mineralization of BV3 increases steadily with irradiation time up to a maximum of 70 %. This level of mineralization is lower than that of the photo-Fenton-like mineralization of phenol in presence of Cu-iminodisuccinic acid in which 95 % mineralization was realized in 60 min [16].

The chemical reactions involved in the generation of oxidizing radicals in the Cu(I) photo-Fenton-like degradation of BV3 are given by chemical equation (I) to (IV) [17]. Reaction (V) shows how the BV3 is converted to mineralization products such as CO_2, water and mineral ions.

(I) $Cu^+ + H_2O_2 \rightarrow Cu^{2+} + \bullet OH + OH^-$

(II) $Cu^{2+} + H_2O_2 \rightarrow Cu^+ + \bullet OOH + H^+$

(III) $Cu^{2+} + \bullet OOH \rightarrow Cu^+ + H^+ + O_2$

(IV) $O_2^{\bullet-} + Cu^{2+} \rightarrow Cu^+ + O_2$

(V) BV3 + ($\bullet OH$, $\bullet OOH$, $O_2^{\bullet-}$) → Mineralization products

Reaction (II) is accelerated by increasing pH [18]. This is perhaps why a high pH in this study resulted in the best performance of the photo-Fenton-like system. The degradation of BV3 was evaluated using pseudo-first-order and pseudo-second-order kinetic schemes. The parameters of these kinetic models are shown in Table 4. The Table clearly shows consistency with pseudo-first-order kinetics described by equation 4.

$$\ln C_o = \ln C_t - kt \qquad (4)$$

Where, C_o and C_t are concentration of the dyes at time 0 and at time t. The k is the Pseudo order first order rate constant and t is the time in minutes.

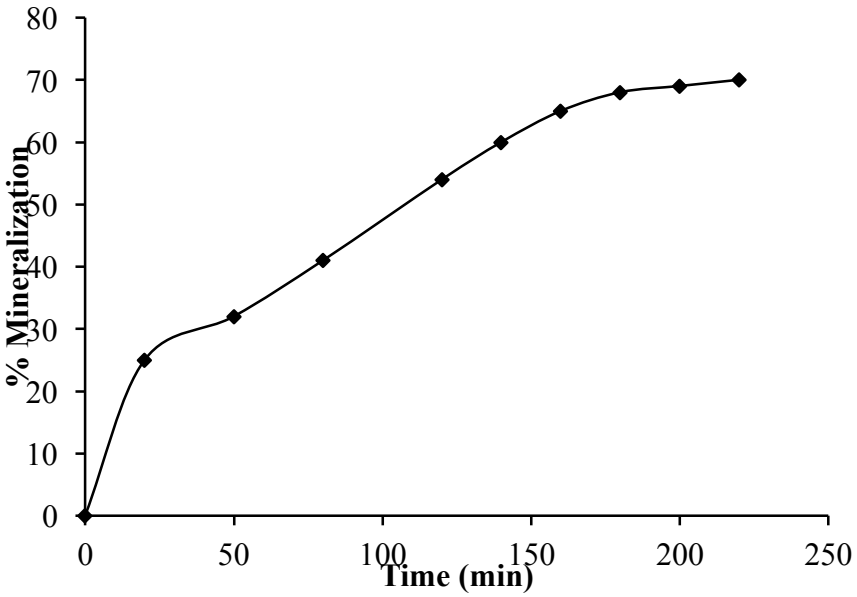

Figure 4: A graph showing the percentage mineralization of BV3 versus time at optimized conditions.

Table 4: Kinetics parameters of BV3 photo-Fenton-like degradation.

Kinetic model	Rate constant	R-squared
Pseudo first-order	0.143 min^{-1}	0.997
Pseudo second-order	0.026 $Lmg^{-1}min^{-1}$	0.890

The IR spectral study was employed to monitor the disappearance of BV3 functional groups upon copper (1) photocatalytic degradation. The strong bands at 1577 and 1480 in Figure 5a indicate the presence of benzene C=C stretch. Annihilation of these peaks (Figure 5b) is evidence for the opening or BV3 rings en route degradation. The peak at 1160 cm^{-1} represents C-N stretch [19]. The two peaks at 760 and 720 cm^{-1} in Figure 5a represent C-H bend of benzene. The appearance of the strong absorption bands at 3321 and 1639 (Figure 5b) confirm the formation of smaller molecules consisting of a secondary amide N-H and/or alkene-based C=C bonds as degradation products.

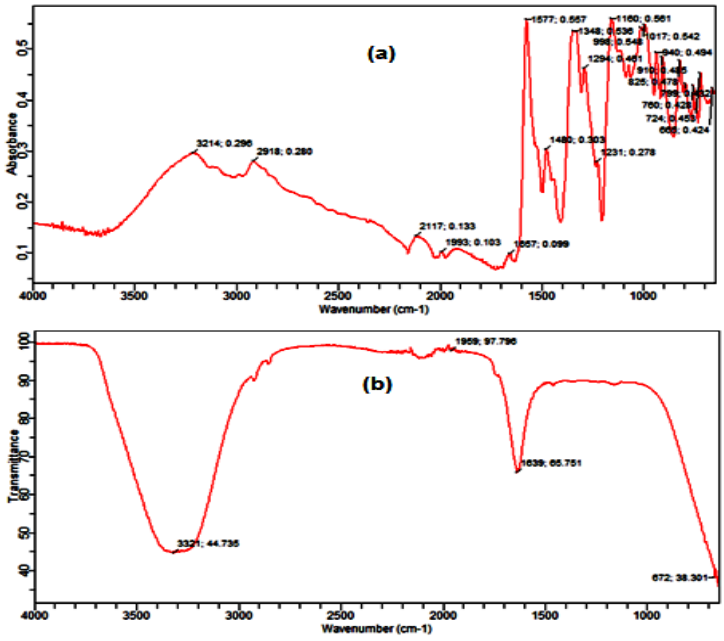

Figure 5: Fourier transform infrared spectra of BV3 before degradation (a), after degradation (b).

Conclusion

Successful copper (I) photo-Fenton-like degradation of aqueous solutions of BV3, for the first time. The homogeneous catalytic degradation process does not significantly depend on the initial concentration of the Basic Violet 3 dye but pH, H_2O_2 and Cu(I) amounts. It has been established that even at alkaline pH photo-Fenton-like degradation can be maximized. Inorganic anion oxidants such as BrO_3^- and ClO_3^- do not affect the Box-Behnken-optimized degradation of BV3.

References

1. S. Kalal, K. Chanderia, K. Meghwal, N.S. Chouhan, R. Ameta, P.B. Punjabi, *Indian J. Chem. Technol.*, 22 (2015) 148-154.
2. Xu, X.R., Li, H.B., Wang, W.H., Gu, J.D. *Chemosphere*, 59 (2005) 893-898.
3. C. Chen, C. Lu, *J. Phys. Chem. C*, 111 (2007) 13922-13932.
4. F. Rehman, M. Sayed, J. A. Khan, H. M. Khan, *J. Chil. Chem. Soc.*, 62 (2017) 3359-3364.
5. F. Rehman, M. Sayed, J.A. Khan, L.A. Shah, N.S. Shah, H.M. Khan, R. Khattak, (2018) 1-16. https://doi.org/10.1515/zpch-2017-1099
6. S.A. Mansour, M.A. Tony, A.M. Tayeb, *Appl. Sci.*, 1 (2019) 265.
7. A. Hassani, C. Karaca, S. Karaca, A. Khataee, O. Açışl, B. Yılmaz, *Ultrason.Sonochem.*, 42 (2018) 390-402
8. R.E. Palma-Goyes, F.L. Guzmán-Duque, G. Peñuela, I. González, J.L. Nava, R.A. Torres-Palma, *Chemosphere*, 81 (2010) 26–32.
9. A. Serra-Clusellas, L. De Angelis, C.-H. Lin, P. Vo, M. Bayati, L. Sumner, Z. Lei, N. Braga, L.M. Bertini, J. Mazza, L.R. Pizzio, J.D. Stripeikis, J.A. Rengifo-Herrera, M.M. Fidalgo de Cortalezzi, *Water Res.*, 144 (2018) 572-580.
10. L. Lyu, L. Zhang, C. Hu, Chem. Eng. J., 274 (2015) 298–306.
11. H.-J. Fan, S.-T. Huang,W.-H. Chung, J.-L. Jan, *J. Hazard. Mater.*, 171 (2009) 1032–1044.
12. K.M. Ranch, F.A. Maulvi, M.J. Naik, A.R. Koli, R.A. Parikh, D.O. Shah, *Int. J. Pharm.*, 554 (2019) 264-275.
13. F. Ay, E.C. Catalkaya, F. Kargi, *J. Hazard. Mater.* 162 (2009) 230–236
14. Evonic, The Modern Chemist's Guide to Hydrogen Peroxide and Peracetic Acid, c&en e-books, American Chemical Society, 2018.
15. F.A. Alshamsi, A.S. Albadwawi, M.M. Alnuaimi, M.A. Rauf, S.S. Ashraf, *Dyes Pigm.*, 74(2007)283-287.
16. A. Fiorentino, R. Cucciniello, A. Di Cesare, D. Fonaneto, P. Prete, L. Rizzo, G. Corno, A. Proto, *Water Res.*, 146 (2018) 206-215.
17. D.A. Nichela, A.M. Berkovic, M.R. Costante, M.P. Juliarena, F.S.G. Einschlag, *Chem.Eng. J.*, 228(2013)1148–1157.
18. H.-J. Lee, H. Lee, C. Lee, *Chem. Eng. J.*, 245 (2014) 258-264.
19. J. Coates, Interpretation of Infrared Spectra, A Practical Approach. In: Encyclopedia of Analytical Chemistry, R.A. Meyers eds., Wiley & Sons Ltd, 2000

(2019) ; http://www.jmaterenvironsci.com